Development 129, 3469-3478 (2002)
Printed in Great Britain © The Company of Biologists Limited 2002
DEV2810

poirot, a new regulatory gene of *Drosophila oskar* acts at the level of the short Oskar protein isoform

Rita Sinka[1], Ferenc Jankovics[1], Kálmán Somogyi[1], Tamás Szlanka[1], Tamás Lukácsovich[2] and Miklós Erdélyi[1,*]

[1]Institute of Genetics, Biological Research Center of the Hungarian Academy of Sciences, H-6701 PO Box 521, Szeged, Hungary
[2]Institute of Biochemistry, Biological Research Center of the Hungarian Academy of Sciences, H-6701 PO Box 521, Szeged, Hungary
*Author for correspondence (e-mail: erdelyim@nucleus.szbk.u-szeged.hu)

Accepted 12 April 2002

SUMMARY

Embryonic germ cell formation and abdomen development in *Drosophila* requires localisation and site specific translation of *oskar* mRNA in the posterior part of the oocyte. Targeting of *oskar* function to the posterior pole of the oocyte needs a large set of proteins and RNAs, encoded by posterior group genes. Consequently, mutations in the posterior group genes can result in embryos without abdomens and/or germ cells. During a systematic *hobo*-mediated mutant isolation screen, we identified *poirot,* a novel posterior group gene, owing to its germ cell-less phenotype. We show that the lack of *poirot* activity dramatically decreases OSK protein levels, without affecting the *oskar* mRNA distribution. In *poirot* mutant oocytes, delocalised OSK protein is observed, indicating that wild-type *poirot* has a role in the anchoring process of the OSK protein at the posterior pole. Furthermore, we demonstrate that *poirot* acts in an isoform-specific manner, only the short OSK isoform is affected, while the long OSK isoform remains at wild-type levels in *poirot* mutants.

Key words: *Drosophila*, Oogenesis, Oskar, Germ plasm, Posterior group, Poirot

INTRODUCTION

The embryonic polarity of many organisms is defined by maternally provided determinants that are localised in the oocyte during egg development. Localisation and the subsequent site-specific translation of mRNAs provides one of the mechanisms that restrict the biological functions of determinants to specific cytoplasmic regions within the oocytes. This type of regulation has been studied most extensively in *Drosophila melanogaster*, as the anteroposterior and the dorsoventral embryonic body axes, and germline differentiation are governed by maternally provided localised determinants.

Post-transcriptional regulation of the localised maternal determinants is achieved by different molecular mechanisms. For example, the anterior morphogen *bicoid* (*bcd*) is translated only after fertilisation and its translation is regulated by cytoplasmic polyadenylation, a common mechanism of maternal mRNA regulation (Salles et al., 1994). Translation of the posterior morphogen *nanos* (*nos*), however, is independent of polyadenylation, and is subject to a more complex regulatory process. Unlocalised bulk cytoplasmic *nos* mRNA is repressed, but localisation of the *nos* mRNA by components of the posterior localised germ plasm activates its translation by preventing the interaction of *nos* mRNA with translational repressors (Dahanukar et al., 1999; Dahanukar and Wharton, 1996; Smibert et al., 1996). Gurken, the key organiser of the dorsoventral polarity of the developing egg and embryo, is also controlled by both positive and negative regulators. According to a recent model reviewed by Cooperstock and Lipshitz (Cooperstock and Lipshitz, 2001), *grk* mRNA is bound by cytoplasmic translation repressor molecules, but in the anterodorsal corner of the oocyte, where *grk* is functional, positive translational regulators relieve the effect of repressors. Finally, the post-transcriptional regulation of *oskar* (*osk*), the key component of the germ plasm assembly, is an even more complex process. Besides repression-derepression events that are similar to the *grk* and *nos* regulation, the OSK protein itself has a positive self-regulatory function. Additionally, it has been shown that the *osk* mRNA is subject to cytoplasmic polyadenylation (Chang et al., 1999). The complexity of its regulation makes *osk* one of the most attractive subjects for the analysis of gene regulation in *Drosophila melanogaster*.

osk mRNA is transcribed exclusively in the nuclei of nurse cells and then transported into the developing oocyte (Ephrussi et al., 1991; Ephrussi and Lehmann, 1992; Smith et al., 1992). Initially, during oocyte development, the *osk* transcript is uniformly distributed (stages 1-6), then it is transiently localised (stage 7) to the anterior pole, and subsequently (after stage 8) to the posterior pole, where OSK protein is first translated. Here, it defines the place of germ cell and abdomen formation. (Ephrussi et al., 1991; Kim-Ha et al., 1991). It has also been shown that, although *osk* mRNA is concentrated at the posterior pole, a significant amount of the *osk* transcript

remains unlocalised (Bergsten and Gavis, 1999). This clearly indicates that mRNA localisation alone is not sufficient for the precise restriction of *osk* function to the most posterior part of the oocyte; instead, the translation and post-translational regulation ensures the wild-type spatial restriction of *osk* activity.

Translational regulation of *osk* mRNA involves the activity of repressors, derepressors, translational activators and the OSK protein itself. It has been demonstrated that unlocalised *osk* is translationally repressed. Three RNA-binding proteins *Bruno* (*Bru*), *apontic* (*apt*) and *Bicaudal-C* (*Bic-C*) have been identified, which play a role in this repression (Kim-Ha et al., 1995; Webster et al., 1997; Lie and Macdonald, 1999; Saffman et al., 1998). Translational activation of posteriorly localised *osk* mRNA is achieved by derepressors that can override the effect of negative regulators. The 5′ region of *osk* mRNA contains a derepressor element, whose deletion prevents translation of posteriorly localised *osk* mRNA (Gunkel et al., 1998). By in vitro RNA-binding assays, two protein species p50 and p68 were identified that specifically bind to this derepressor element (Gunkel et al., 1998). Structural and functional analysis of the dsRNA-binding protein *staufen* (*stau*) revealed that its dsRBD5 domain is involved in the derepression of *osk* mRNA at the posterior pole (Micklem et al., 2000). Several other positive trans-regulators of the *osk* translation have also been identified. *Orb*, which is homologous to the *Xenopus* cytoplasmic polyadenylation element binding protein (CPEB) activates *osk* mRNA translation, most probably by promoting polyadenylation (Chang et al., 1999). *aubergine* (*aub*) enhances *osk* translation through an interaction with 3′UTR and sequences upstream of 3′UTR of *osk* mRNA (Wilson et al., 1996). Translation of *osk* mRNA also requires the DEAD box RNA helicase, Vasa (VAS), which has been shown to interact with BRU; thus, VAS may activate *osk* mRNA translation by blocking *Bru* function. However, it has been shown that VAS is required for the translation of *osk* mRNA in the absence of BRU repression, which suggests that *vas* overcomes not only *Bru*-mediated repression (Rongo et al., 1995; Webster et al., 1997; Markussen et al., 1995).

As *osk* translation depends on posterior localisation of *osk* mRNA, genes that are involved in *osk* mRNA localisation also indirectly regulate *osk* translation (Cooperstock and Lipshitz, 2001). Investigation of *osk* mis-sense and nonsense mutations has revealed that the OSK protein is required to maintain *osk* mRNA at the posterior pole (i.e. a positive-feedback mechanism exists) (Ephrussi et al., 1991; Kim-Ha et al., 1991; Markussen et al., 1995; Rongo et al., 1995). *osk* mRNA is translated into long OSK (71 kDa) and short OSK (55 kDa) proteins, of which the short isoform undergoes phosphorylation, which produces a 57 kDa protein (Markussen et al., 1995; Rongo et al., 1995). Phenotypic analysis of in vitro constructed *osk* transgenes, which express either short or long OSK proteins, has demonstrated that both isoforms are effective in maintaining *osk* mRNA at the posterior pole, but only the short OSK is able to organise germ plasm assembly (Breitwieser et al., 1996; Markussen et al., 1995). Several other *osk* regulatory genes, which have a role in mRNA localisation, translational repression, derepression and activation, have been identified; however, no factors that play a role in anchoring OSK protein to the posterior pole have yet been described.

If *osk* regulation occurs correctly, the function of the OSK protein is restricted to the posterior pole, where it recruits components of the germ plasm. Absence of OSK protein from the posterior pole leads to posterior phenotypes, when embryos develop without abdomens and germ cells. Furthermore, *osk* gene dose experiments have shown that *osk* is a limiting factor in determining the number of germ cells and NOS protein activity (Ephrussi and Lehmann, 1992; Gavis and Lehmann, 1994; Smith et al., 1992). The two related *osk* phenotypes (germ cell-less and abdomenless) have different sensitivity to the germ plasm concentration. Moderate level of the localised OSK protein results in a failure of germ cell formation, while abdomen formation is intact (Erdélyi et al., 1995; Jankovics et al., 2001). Thus, the maternal effect germ cell-less, which is also referred to as the grandchildless (gs) phenotype, provides a very sensitive genetic selection system by which *osk* regulatory genes can easily be identified.

In this paper, we report on the isolation and characterisation of a novel *osk* regulatory gene *poirot* (*prt*). We show that the lack of *prt* activity results in delocalisation of OSK protein from the posterior pole but has no effect on *osk* mRNA. Our results show that the *prt* mutant allele acts in an isoform-specific manner, only the short OSK isoform is affected while the long OSK isoform remains at the wild-type level.

MATERIALS AND METHODS

Fly strains and genetics

Flies were kept on standard yeast-cornmeal medium. Crosses were performed at 25°C unless otherwise stated. Oregon-R flies were used as wild type. *Df(2R)XTE58*, *Df(2R)XTED1*, *Df(2R)l4* and *Df(2R)JP1* and $T(2;3)Ta^{L}$ mutant chromosomes are described by Underwood and co-workers (Underwood et al., 1990). Other mutations and balancer chromosomes are described by Lindsley and Zimm (Lindsley and Zimm, 1992). Seven hundred and fifty homozygous viable *hobo* H[pHlw2] (Smith et al., 1993) insertion lines were screened in total for grandchildless phenotypes from an unpublished mutant collection from the laboratory of István Kiss (kindly provided by István Kiss's laboratory). Homozygous females from each mutant line were crossed with Oregon-R, wild-type males and germ cell-less phenotypes of their adult progeny were recognised by hand dissection. prt^{gs} allele was identified as an incomplete penetrant grandchildless mutation.

Hobo element remobilization

H[pHlw2] *hobo* insertion was remobilised from *prt* gene by the *hobo* transposase bearing P[ry^{+} HBL1] transgene (Calvi et al., 1991; Smith et al., 1993). y w/y w; prt^{gs}/*CyO* females were crossed to *CyO* P[ry^{+} HBL1]/*Bc Elp* males. Individual *y w/Y*; prt^{gs}/*CyO* [ry^{+} HBL1] males and *y w/y w*; prt^{gs}/*CyO* P[ry^{+} HBL1] females were crossed to *w/w; SM6b/Sco* and *w/Y; SM6b/Sco* males, respectively. Next, *SM6b* balanced revertant (prt^{gsR}) stocks were established from white eyed *y w/Y;* prt^{gsR}*/SM6b* progeny. Revertants were selected by the loss of the grandchildless phenotype.

Embryonic cuticle preparation

Embryonic cuticle preparations were made as described by Wieshaus and Nüsslein-Volhard (Wieshaus and Nüsslein-Volhard, 1986). Eggs from mutant females were collected, dechorionated with 50% Chlorox bleach, washed, mounted in Hoyer's medium lactic acid 1:1 mixture and cleared for 24 hours at 60°C.

Generation of the PRT polyclonal antibody

The C-terminal coding sequences of *prt* were cloned into pGEX-4T-

1 and Glutatione S-transferase (GST)-fusion proteins were produced in *E. coli* strain BL21 using standard induction conditions. GST-PRT proteins were purified by Glutatione Sepharose 4B, according to the manufacturer's instructions (Amersham Pharmacia Biotech). Polyclonal antibody was raised in rabbit against bacterially expressed and purified GST-PRT.

Western blot analysis

Hand dissected ovaries were sonicated in 10 volumes of extraction buffer (6 mM Tris-Cl, pH=6.8, 6.4% glycerol, 2% SDS, 100 mM DTT and Bromophenol Blue). Extract equivalent of approx. one pair of ovaries was loaded per lane on 10% SDS-PAGE gels. Proteins were transferred to PVDF membrane (Amersham) at ~7 V/cm for 12-18 hours in cold transfer buffer (20% methanol, 25 mM Tris-Cl, 192 mM Glycine). BioRad Kaleidoscope Prestained Standards were used as molecular weight markers. Blots were blocked using 5% dry milk in TTBS, and incubated with anti-OSK antibody diluted 1:1000, anti-PRT antibody diluted 1:3000, anti-γ-tubulin (Sigma) antibody diluted 1:1000 and in TTBS 5% dry milk. The membrane was washed in dH_2O, TTBS and incubated with peroxidase-conjugated goat anti-rabbit secondary antibody in 5% dry milk in TTBS (Jakson Immuno Research Laboratories). Signals were detected with enhanced chemiluminescence.

Cloning and transgenes

Flanking sequences of the *prt^{gs} hobo* insertion were amplified by adapter-PCR technique. Genomic DNA was cleaved with *Aat*II restriction enzyme and ligated to a synthetic *Aat*II adapter composed of 5′-ACCAGCTAAACGCAACCCTAAGACGT-3′ (AD1) and 5′-CTTAGGGTTGCGTTTAGCTGGT-3′ (AD2) synthetic oligomers. DNA fragments were amplified with *hobo* element-specific *lacZ*-F1 (5′-GGATAGGTTACGTTGGTGTAG-3′) and AD1 primers. One tenth of the PCR products was reamplified using a pair of nested primers: lacZ-F2 (5′-TCGCACTCCAGCCAGCTTTCCGG-3′) and AD1. PCR products were separated by agarose gel electrophoresis, purified from the gel and subcloned into a pBR322 cloning vector. The insert was sequenced with a ABI Prism 310 Sequencer (Perkin Elmer). ORF finder and Blast programs (BDGP BLAST service) were used to analyse the sequences. The UASp-*prt* construct was generated by inserting the 2.2 kb HL01519 EST of BDGP (Rubin et al., 2000) into a pUASp vector (Rorth, 1998) and transforming into the *Drosophila* germline, according to the standard protocol (Rubin and Spradling, 1982). The UASp-*prt-gfp* construct was made by inserting the coding region of *prt* cDNA (HL01519) in frame to GFP in β-globin 2×GFP vector (J. Knoblich, personal communication) and *prt-gfp* cloned into *Drosophila* pUASp vector. Stable w/w; UASp-*prt*/TM3 transformant lines were established and crossed to nosGAL4-VP16 (Van Doren et al., 1998) germline-specific drivers at the *prt^{gs}* homozygous background.

RT-PCR

Total RNA was Trizol extracted (Gibco BRL). cDNA was synthesised on 3 μg of total RNA template with M-MuLV Reverse Transcriptase (Fermentas) and random hexanucleotid primers (Amersham). Two primers complementary to the first and fourth *prt* exons (PRT1F, 5′-TAATACCTGCTGCTGTTACCCGCA-3′; PRT4R, 5′-GGCCCCCT-AAGGTTGCTCACTATT-3′) were used in PCR amplifications and a control PCR was performed using *rp49* primers (rp49 forward, 5′-GCATACAGGCCCAAGATCCGT-3′; rp49 reverse, 5′-CAATCT-CCTTGCGCTTCTTG-3′) in the same reaction. The chimaeric *prt-mini-white* splice product was amplified by PRT1F and *mini-white* 3. exon specific (white3R: 5′-GTGTGCTGACATTTGCTGA-3′) primers. RT-PCR products were separated by agarose gel electrophoresis. Results were evaluated by using the Gel Base program. RT-PCR products were direct sequenced with ABI Prism 310 Sequencer (Perkin Elmer).

Detection of proteins in wholemount

Bleach dechorionated embryos and dissected ovaries were collected in PBS. Ovaries were fixed for 10 minutes in a mixture of 1 volume fixation buffer (100 mM KH_2PO_4 pH=6.8, 450 mM KCl, 150 mM NaCl, 20 mM $MgCl_2$), 3 volumes dH_2O and 2 volumes 16% formaldehyde. Embryos were fixed for 12 minutes in a mixture composed of one volume of fixation buffer (0.1 M PIPES, 2 mM $MgSO_4$, 1 mM EGTA pH=6.8), 1/10 volume of 37% formaldehyde and one volume of heptane. The aqueous phase was removed and one volume methanol was added. Ovaries and devitellinized embryos were washed in PBT for 2×20 minutes and blocked for 1 hour in blocking solution (PBS plus 0.1% BSA, 0.1% Triton X-100, 5% normal goat serum and 0.02% NaN_3). Ovaries and embryos were then incubated overnight with rabbit anti-OSK primary antibody (1:500 dilution) or rabbit anti-STAU (1:2000 dilution) and rat anti-VAS antibody (1:750 dilution) in blocking solution. This was followed by a 4×30 minute wash in PBT and an hour wash in blocking solution. The final incubation was with a fluorescein-conjugated anti-rabbit secondary antibody diluted 1:200 (Jakson Immuno Research Laboratories) or anti-rat peroxidase-conjugated secondary antibody 1:100 (Amersham) in blocking solution for 2 hours, following which, ovaries and embryos were washed for 4×30 minutes in PBT. The VAS signal was visualised by DAB detection. Preparations were mounted in 80% glycerol and 4% n-propyl-gallate. The ovaries and embryos were analysed with Zeiss Axioscope II microscope, Axiocam CCD camera and Zeiss LSM 410.

RNA in situ hybridisation

Digoxigenin-labelled DNA probe was synthesised using a Dig DNA labelling kit (Boehringer Mannheim). The *osk* DNA probe corresponds to the 2.1 kb *Sac*I fragment of *osk* cDNA (Ephrussi et al., 1991). Hybridisation was carried out as described in by Ephrussi and co-workers (Ephrussi, 1991). Hybridisation signals were detected using the Dig Detection kit (Boehringer Mannheim). Hybridisation was analysed with interference contrast microscopy (Zeiss Axioscope II).

RESULTS

prt^{gs} mutation interferes with embryonic germ cell and abdomen differentiation

Seven hundred and fifty viable autosomal *hobo* insertion lines were screened and a single line (*prt*) was found, of which the females, homozygous for the *hobo* insertion, exhibited the grandchildless (gs) phenotype. *prt^{gs}*/*prt^{gs}* females, when mated with wild-type males, gave rise to 70% agametic adult progeny. This incomplete penetrant *gs* mutation frequently resulted in mosaic gonads. In 10% of the progeny, mosaic pairs of gonads were found when one ovary or testis was agametic, while the other gonad was full of developing egg primordia (data not shown). This observation suggests that the mutation interferes with the number but not the function of adult germ cells, and the reduction of germ cells happened at an early development phase. Indeed, we observed dramatically reduced or completely missing germ cells in 70% of embryos from homozygous *prt^{gs}* females (Fig. 1A,B). Comparing the penetrance of the embryonic and adult phenotypes, we concluded that the germ cell-less phenotype observed in adulthood is a sole consequence of the failure in the earliest steps of embryonic germ cell development. This was further confirmed by the stronger phenotype observed at 18°C. Five percent (n=357) of the embryos originated from *prt^{gs}*/*prt^{gs}* females and wild-type males showed variable but characteristic

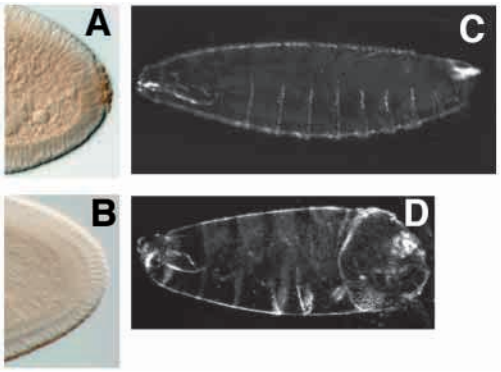

Fig. 1. Embryonic germ cell-less (grandchildless) and abdomenless phenotypes of *prt^{gs}* mutant embryos. (A) Wild type, early cellular blastoderm embryo with embryonic germ cells at the posterior at 25°C, as shown by staining with anti-Vasa antibody, and (B) embryo without embryonic germ cells from a *prt^{gs}*/*prt^{gs}* mother. (C,D) Cuticle preparation of wild-type and mutant, *prt^{gs}*/*prt^{gs}* female originated embryo at 18°C. (C) Wild-type embryo with normal abdominal segmentation, and (D) a mutant embryo from *prt^{gs}*/ *prt^{gs}* mother with a weak abdomenless phenotype. All embryos oriented anterior leftwards, dorsal upwards.

abdomenless phenotypes (Fig. 1C,D) coupled with a slightly elevated, 85% adult gs phenotype at 18°C. This indicates that the origin of the embryonic germ cell-less phenotype is mutual with that of the abdomen defect and this is a consequence of the misfunction of the early (maternally) acting posterior gene hierarchy.

However, when *prt^{gs}*/*prt^{gs}* females were mated with *prt^{gs}*/*prt^{gs}* males, the resulting maternal and zygotic mutant progeny exhibited a more complex mutant phenotype. Abdominal defects characteristic to posterior group mutants were coupled with variable embryonic defects manifested in cuticle holes that were most frequently observed in the head region (data not shown). By crossing to wild-type males, the paternal rescue of zygotic cuticle defects allows us to investigate only the maternal effect of *prt* mutations. We also observed that egg-laying capacity of the *prt^{gs}* homozygous females was only 33% and 30% of wild-type females at 25 and 18°C, respectively, indicating that besides its zygotic function *prt* has another, early function during oogenesis (Table 1). In this paper we concentrate on the *prt* gene function in the germ cell formation.

Genetic analysis classifies *prt^{gs}* as a null allele

The *prt^{gs} hobo* insertion was mapped to the 51 D6-12 chromosomal region by in situ hybridisation. Uncovering deficiencies [*Df(2R)XTE58*, *Df(2R)Jp1* and *Df(2R)l4*] from this region did not complement the *prt^{gs}* grandchildless phenotype. We observed that penetrance of *prt^{gs}* homo- and hemizygous phenotypes was almost identical (70% and 66%, respectively), indicating that *prt^{gs}* is most likely to be a null allele. With other deficiencies [*Df(2R)XTED1* and *Df(2R)X9*] from this region, which did complement the grandchildless phenotype, the *prt^{gs}* mutation was mapped to the 51D12-51E5-7 chromosomal region.

To prove that the *hobo* insertion is responsible for the grandchildless phenotype, we remobilised the insertion from the *prt* locus. Out of 455 independent lines, five revertants were isolated by the complete loss of the grandchildless phenotype. The revertants have proved that *prt^{gs}* is a *hobo*-induced mutation, and this made the gene accessible for molecular analysis.

PRT protein shows extended homology to *Sab*, a human SH3 domain-binding protein

In order to clone the *prt* gene, a flanking genomic DNA sequence of the *hobo* insert was amplified by an adapter PCR strategy (see Materials and Methods). The resulting 1.5 kb PCR *hobo* flanking sequence was identical to a part of the 72 kb sequenced P1 phage, DS04940, which maps to the 51D-E region (Hartl et al., 1994). The insertion point was precisely mapped at 34,569 bp in P1 phage sequence, in the first intron of the CG7761 (Adams et al., 2000; Rubin et al., 2000) annotated gene (Kimmerly et al., 1996) that we named *poirot* (*prt*). We collected four available partially sequenced CG7761 EST-s, completed the sequence of HL01519 and determined the exon-intron boundaries within the genomic DNA (Fig. 2A).

In order to prove that the *prt* gene is responsible for the grandchildless phenotype we performed a phenotypic rescue experiment. HL01519 cDNA was cloned into a pUASp vector, transformed into *Drosophila* and expressed exclusively in the female germline by the nosGal4Vp16-UASp expression system (Rorth, 1998; Van Doren et al., 1998). The UASp-HL01519 transgene completely rescued the phenotype of *prt^{gs}* homozygous females when nosGAl4Vp16 was present. In the absence of GAL4Vp16 trans-activation, we observed characteristic grandchildless phenotype. Based on this result, we concluded that the *prt^{gs}* mutation is germline dependent and the HL01519 cDNA contains the entire *prt* function.

Conceptual translation of *prt* cDNA predicted a 477 amino acid protein that shows extensive homology to human and mouse Sab proteins (Fig. 2B) (Matsushita et al., 1998; Yamadori et al., 1999). Sequence analysis revealed that the 257 amino acid N-terminal part of PRT shows significant homology to the Sab protein family. PRT shares 48% identity and 66%

Table 1. Abdomenless and germcell-less phenotype and egg-laying capacity of *prt^{gs}* mutants

	Embryo with posterior phenotype at 18°C*		Adult with germcell-less phenotype at 18°C†		Adult with germcell-less phenotype at 25°C†		Egg-laying capacity at 25°C‡		Egg-laying capacity at 18°C‡	
	Number	%	Number	%	Number	%	Number of females	Eggs/ female/day	Number of females	Eggs/ female/day
Wild type	331	0	160	0	100	0	100	14	331	8.275
prt^{gs}/*prt^{gs}*	357	5.04	162	4.60	116	70	100	3.2	357	2.47

*The posterior phenotype was visualized by embryonic cuticle preparation.
†The adult germcell-less phenotype was determined by dissection.
‡The egg-laying capacity of 5-day-old females was monitored over 3 days. The average eggs/female/day values are indicated.

similarity to the human, and 45% identity and 63% similarity to murine Sab proteins, while the C-terminal region did not show any significant homology to known proteins. Sequence comparisons also identified a predicted *C. elegans* K03E6.7 (38% identity and 56% similarity) and a *Drosophila* CG14408 (38% identity and 54% similarity) homologue of the 252 amino acid N-terminal part of the PRT protein. The N-terminal region of human Sab contains an unconventional SH3-binding domain, which preferentially binds to the SH3 motif of Bruton's Tyrosine kinase (Btk) protein (Matsushita et al., 1998). Interestingly, the 32 amino acids long SH3-binding domain of human Sab shows 48% identity and 73% similarity to the corresponding part of PRT, indicating that the two proteins may have conserved functions.

A

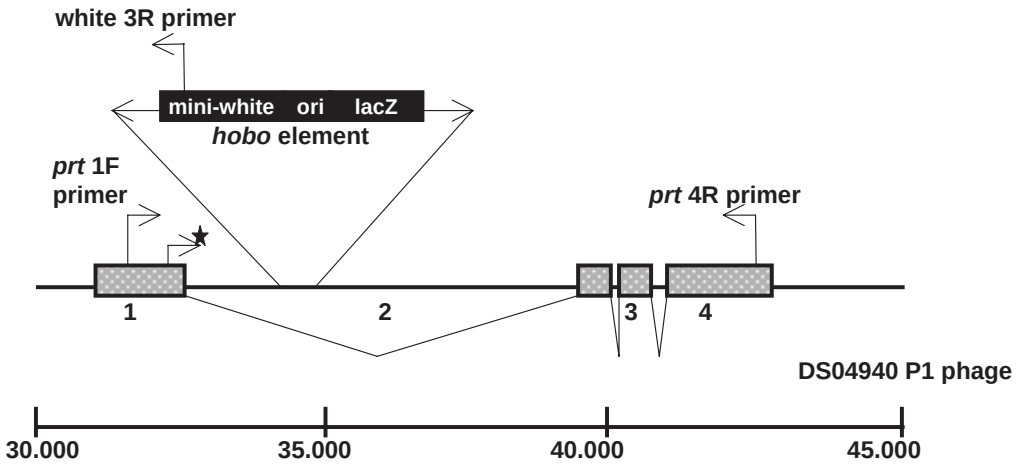

B

```
                          *       20        *       40        *       60        *       80        *
human Sab          : ------------------MEQGLEEEEE------VDPRIQGELEKLNQSTDDINRRETELEDARQKFRSVLVEATVKLDELVKKIGKAVE :  66
mouse Sab          : ------------------MEQGLEEEEEE-----VDPRIQGELEKLNQSTDDINRRETELEDARQKFRSVLVEATVKLDELAKKIGKAVE :  67
Poirot             : ------------------MSSAEDGE--------LDPQIQIELENLNSATDEINKLEIELEEANSTFRILLNESTRRLKVSSKKLGNCIE :  64
C. elegans K03E6.7 : MDETATSSEVTETFVSDPTTRQFEEDGHPPLETRHLNMIHEELEKLNISTDVINKMEVQLDLARADFRETQVQWSEKLKELSKQYSSQIA :  90

                           100       *       120       *       140       *       160       *       180
human Sab          : DSKPYWEARRVARQAQLEAQKATQDFQRATEVLRAAKETISLAEQRLLED-DKRQFDSAWQEMLNHATQRVMEAEQTKTRSELVHKETAA : 155
mouse Sab          : DSKPYWEARRVARQAQLEAQKATQDFQRATEVLRAAKETISLAEQRLLED-DKRQFDSAWQEMLNHATQRVMEAEQTKTRSELVHKETAA : 156
Poirot             : KARPYYEALDKAREAQIECQKAAVKFQRANEIHAAAKETVALAEQRFMSNSHEWQFDNAWQEMLNHATQKVMDAETQKADCHAEHQRLTK : 154
C. elegans K03E6.7 : KARPFYELKIKERSLREESQKAAERFERATSILGIAKQQVSLTQESLSRQ---TSVLPECLEVLNHHIQRVREVEEERTAAESLHASKAH : 177

                          *       200       *       220       *       240       *       260       *
human Sab          : RYNAAMGRMRQLEKKLKRAINKSKPYFELKAKYYVQLEQLKKTVDDLQAKLTLAKGEYKMALKNLEMISDEIHERRR---SSAMGPRG-C : 241
mouse Sab          : RYNAAMGRMRQLEKKLKRAINKSKPYFELKAKYYVQLEQLKKTVDDLQAKLALAKGEYKAALKSLERISDEIHERRR---SNAMGPRG-C : 242
Poirot             : LFNAAEQKLQQLEDRFRRSINKSRPYFEEKQVCQDQLQTQKNRIQELQQQVAGAKSTYSTALRNLERISEDIHRQRGDF-PTPPGPRE-P : 242
C. elegans K03E6.7 : AMLHLAEKIRAMEKDNRYAIKKSRLYFEKRLEFTKILEAQKATILCLEAEVRQKKNDYTTSLRNLERISERIHEERS--TGSLESAVSSD : 265

                           280       *       300       *       320       *       340       *       360
human Sab          : GVGAE---GSSTSVEDLP---------------GSKP--EPDAIS-VASEAFED--DSCS----------NFVSEDDSE--TQSVSSFSS : 296
mouse Sab          : GVGAE---GSIASVENLP---------------VSKP--EPDAISSVASEAFED--DNCS----------NLVSEDDSE--TQSVSSFSS : 298
Poirot             : GVGAELNSPTSSALPSLPDFQLELEKCDYPSIAGSQM--SLGAKTPQAAAETEDEEDACDYDETGAGELRGVVDERDLEALRQKVKILAV : 330
C. elegans K03E6.7 : QEDQK---SDFKSSESLP---------------GNPPPYAPTAPPPYEDKYIIDK-DDDS------IVLNMIKTEQEEEGEKRNSRSLGS : 330

                          *       380       *       400       *       420       *       440       *
human Sab          : GP-------TSPSE---MPDQFPAVVR------PGSLDLPSPVSLSEFG-----MMFPVLGPR-SEC---SGASSPE--CEVERGDRAEG : 359
mouse Sab          : GP-------TXPSE---MPDQFPAVAR------PGSLDLPSPVSLSEFG-----MMFPILGPR-SEC---SGASSPE--CEVERGDRAEG : 361
Poirot             : RP-------IEGGDGQQQNDVWEHELK------ATVDKLDHLMMLKETAKRQQTNRLKSTEQR-PDS---LGAEALKRHCDVVEV-KVTS : 402
C. elegans K03E6.7 : GVILLAQQLIGNGNS--TEKHNITPPRHGEEADISYHTRPVGLSDGSDNSEVSSLASFNIGDDDTVSKMLMSHSELIKECAAIKIEAISV : 418

                           460       *       480       *       500       *       520       *
human Sab          : AENKTSDK--ANNNRGLSSSS--GSGGSSKSQSSTSPEGQALENRMKQLSLQCSKG-----RD-----GIIADIKMVQIG-- : 425
mouse Sab          : AENKMSDK--ANNNRVLGSTN--GGSGSRSRSQSSTSLESQALETRMKQLSLQCSKG-----RD-----GIIADIKMVQIG-- : 427
Poirot             : CATTASLP--VTPHHQLNHLA--PPTPIKKLQQQLAPLP-SVNVSMRELPLLARLSNELLDRSSAAFGGVRKTLRRRSLE-- : 477
C. elegans K03E6.7 : IAVAKKFQNRQLPKLQVADKFRLPRTPPCKPQIKNSTLI-SLDTFLANQSIVFEISMAVGERGYPFPFLSLECFRRVSGTCR : 499
```

Fig. 2. (A) The structure of the *prt* gene. *prt* contains four exons (1-4) and three introns. The Hobo element is inserted in the first intron of the *prt* gene that corresponds to 34569 bp in the DS04940 P1 phage. The *hobo* insertion is indicated by a triangle. The translation start site is in the first exon, marked by a star. Right-angled arrows show the orientation of the primers *prt* 1F, *prt* 4R and White 3R, which were used in RT-PCR reactions. (B) Multiple alignment of the amino acid sequences of PRT, human and mouse Sab-s, and *C. elegans* K03E6.7. Human and mouse *Sab* have been reported previously (Matsushita, 1998; Yamadori, 1999). The grey background indicates identical residues, and the black background indicates the minimum region required for binding to BTK in the human *Sab* sequence.

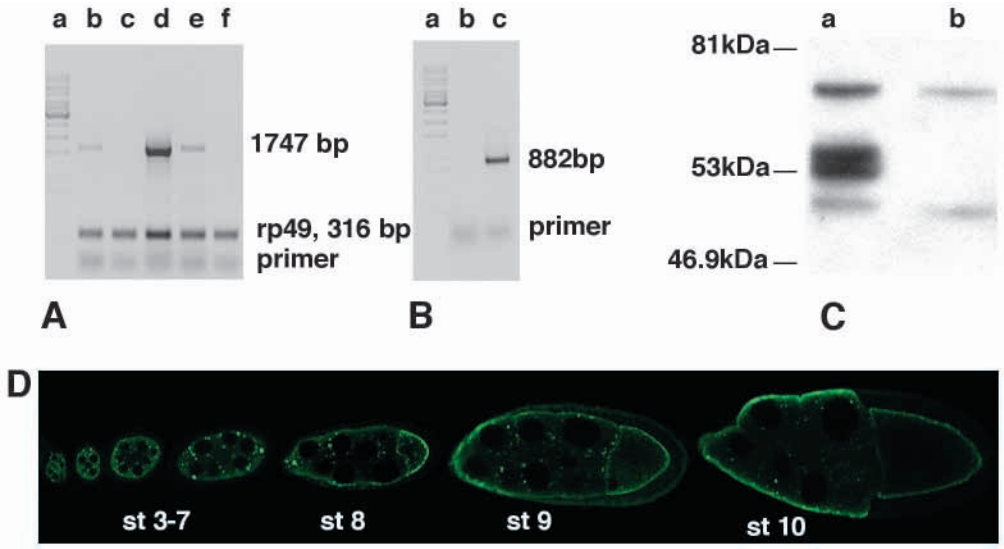

Fig. 3. RT-PCR and western blot analysis of the *prt*^{gs} mutation. (A) Amplification of the 1747 bp *prt* cDNA fragment with *prt* 1F and *prt* 4R (Fig. 4) primers. rp49 primers were used as a template amount control in the same reaction. (Lane a) molecular weight marker (1 kb ladder, Fermentas), (lane b) wild type female, (lane c) *prt*^{gs} female, (lane d) wild-type embryo, (lane e) *prt*^{gs} maternal null embryo originated from a cross of a *prt*^{gs} homozygous female and a wild-type male, (lane f) maternal and zygotic *prt* null embryos, the progeny of *prt*^{gs} homozygous females and males. (B) Demonstration of an aberrant splice variant in the *prt*^{gs} mutant females by RT-PCR. *Prt* 1F and white 3R primers were used in the RT-PCR reaction. (Lane a) molecular weight marker. An 882 bp long RT-PCR product from the aberrant splice species was amplified in the mutant *prt*^{gs} (lane c) but not in the wild type (lane b). (C) Western blot of wild-type (lane a) and *prt*^{gs}/*prt*^{gs} (lane b) ovary extracts. The blot was probed with an antibody against *Drosophila* PRT. A doublet of 53-55 kDa is recognised in ovary extracts from wild-type flies, but not from homozygotes for *prt*^{gs}/*prt*^{gs}. (D) PRT-GFP fusion protein distribution in different stages (st) of developing eggs in wild type.

Intronic *hobo* element insertion resulted in RNA null *prt* allele by forcing an aberrant splicing

In order to find out the consequence of the *hobo* insertion on the *prt* transcription, we performed RT-PCR analyses. Complementary primers to the first, second and fourth exons of the *prt* gene were used to amplify two different regions of the *prt* RNA sequence between exons 1 and 4 and 2 and 4. The 1747 bp PCR product, corresponding to the exons 1-4, was successfully amplified from RNA template of wild-type females, while we did not detect a PCR fragment from the *prt*^{gs} homozygous mutant females (Fig. 3A, lanes b,c). The RT-PCR reaction with exon 2- and exon 4-specific primers also detected no mRNA in the mutant (data not shown). We obtained the same negative results by using RNA templates from both maternally and zygotically mutant *prt*^{gs} embryos (Fig. 3A, lane f). By contrast, RT-PCR analysis of embryos that were only maternally mutant, but fertilised by wild-type male, revealed the presence of a robust zygotic transcript from the paternally inherited wild-type *prt* allele (Fig. 3A, lanes d,e). These data indicated either the complete loss of the *prt* mRNA from the *prt* insertion alelle or the presence of a new, elongated fusion transcript from the mutant chromosome. To exclude one of the above possibilities, we tried to identify possible aberrant splice forms, which would include exons of both the *prt* gene and *hobo* transposon. As the orientation of *mini-white* marker gene in the inserted *hobo* element was the same as that of *prt*, we analysed possible chimaeric splice forms between the *prt* and *mini-white* genes. Using *prt* and *mini-white* specific primers, we were able to amplify a 882 bp long RT-PCR product on RNA template purified from *prt*^{gs} homozygous females (Fig. 3B). We sequenced the PCR product and found that the aberrant splice product contained the first exon of *prt* and the second, third and fourth exon of the *mini-white* gene. As this chimaeric mRNA contained the complete coding sequence of the *mini-white* gene, the active White protein product might be translated from this aberrant splice form.

PRT protein forms aggregates and localises in the subcortical region of the developing oocyte

To identify the distribution of PRT protein in the developing oocyte, we raised a polyclonal rabbit antibody against the PRT protein. Western blot of wild-type ovary protein extracts showed that the anti-PRT antiserum recognised a 53-55 kDa doublet that was absent from the *prt*^{gs} ovary extract (Fig. 3C). Computer analysis of the PRT protein sequence revealed several potential phosphorylation sites, indicating that the 55 kDa PRT protein species could be the result of a post-translational modification. However, the anti-PRT antiserum failed to detect PRT protein in whole-mount ovaries. In both wild-type and *prt*^{gs} mutant ovaries, we obtained a low level uniform staining (data not shown). As an alternative approach to visualise the distribution of PRT protein during oogenesis, we used the UASp/nosGal-Vp16 system (Rorth, 1998; Van Doren et al., 1998) to express a GFP-tagged version of PRT in the *Drosophila* germline. Several independent PRT-GFP transgenic lines were established and assayed for GFP expression after nosGal4VP16 induction. All these lines showed similar GFP expression pattern and rescued the *prt*^{gs} germ cell-less phenotype (Fig. 3D). In early egg chambers, (stages 2-4) PRT-GFP is concentrated in large cytoplasmic aggregates around the nuclei of nurse cells. During stages 4 to 7, this particulate appearance of PRT-GFP is detectable both in nurse cells and oocytes. From stage 8, when the microtubule network of oocytes is reorganised, the PRT-GFP aggregates can be found exclusively in the subcortical region. During stages 9-10, the nurse cells and the oocytes contain similar amounts of PRT-GFP protein. Formerly, it has been reported that the Exuperantia, Me31B, ORB and CUP proteins show similar distribution during egg development to PRT-GFP (Wilsch-Brauninger et al., 1997; Nakamura et al., 2001; Mansfield et al., 2002; Keyes and Spradling, 1997). Thus, we next asked whether PRT was colocalised with any of the above proteins; however, it was not (data not shown).

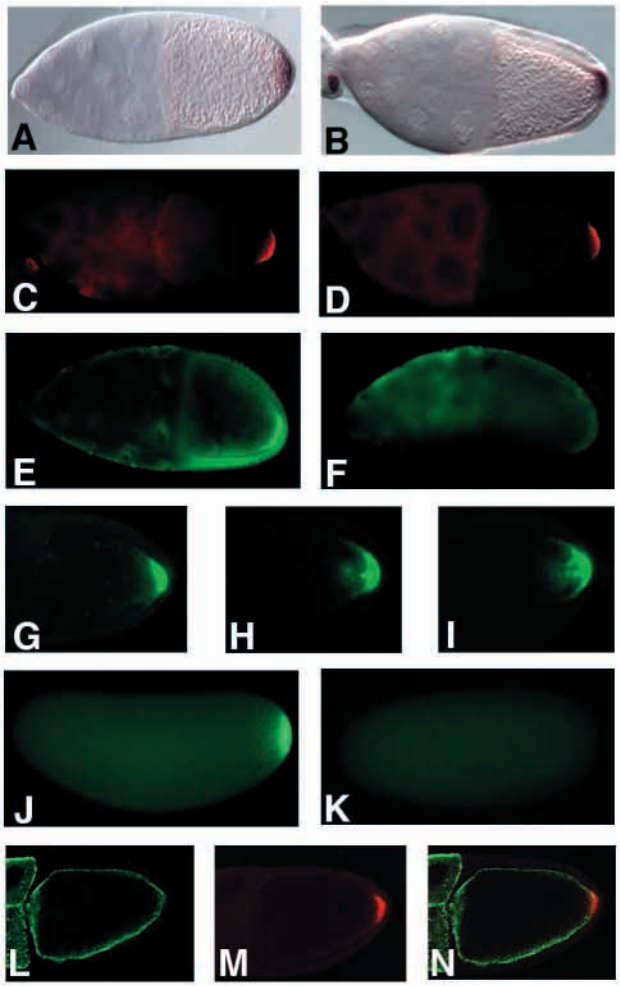

Fig. 4. (A-K) *osk* mRNA, STAU protein is normal in wild type and prt^{gs}/prt^{gs} mutant oocytes. OSK protein shows delocalisation or is missing from the posterior pole in the mutant oocyte and embryo. (L-N) PRT-GFP fusion protein and Osk protein colocalisation in oocyte. (A) *osk* mRNA is localised at the posterior pole in wild type and (B) prt^{gs}/prt^{gs} stage 10 oocytes. (C) STAU is localised at the posterior pole in wild-type and (D) prt^{gs}/prt^{gs} stage 10 oocyte. (E,G) Wild-type OSK localisation at the posterior pole of the stage 10 developing egg, (F) No OSK is detectable in the prt^{gs}/prt^{gs} egg chamber. (H,I) OSK protein is degraded from the posterior of prt^{gs}/prt^{gs} egg chambers, (J) OSK protein has posterior localisation in wild-type embryos, (K) there is no detectable OSK in prt^{gs}/prt^{gs} embryos. (L) PRT-GFP protein is subcortical in stage 10 wild type oocytes, (M) OSK protein is localised to the posterior pole and (N) in this stage they show colocalisation.

Table 2.Oskar protein localisation in prt^{gs} mutant oocytes and embryos

	Normal OSK protein		Mislocalised or no OSK protein	
	Number	%	Number	%
Wild-type stage 10 oocyte	97	95	5	5
prt^{gs}/prt^{gs} stage 10 oocyte	65	61	41	38
Wile-type embryo	81	100	0	0
prt^{gs}/prt^{gs} embryo	4	9	45	91

Oocytes and embryos were stained with an antibody to the OSK protein.

prt^{gs} decreases OSK protein level and results in OSK delocalisation

As prt^{gs} resulted in both germ cell- and abdomenless phenotypes, which are characteristic to mutations of the posterior group genes, we investigated the mRNA and protein distribution of *osk*, the key element of the posterior gene hierarchy. Using RNA in situ hybridisation, we did not observe significantly reduced posterior localised *osk* mRNA in prt^{gs}/prt^{gs} mutant ovaries (Fig. 4A,B). Consistently, an RNA-binding protein, Staufen, which colocalises with *osk* mRNA and thus is used as an *osk* mRNA distribution marker (St Johnston et al., 1991) was found at the posterior pole in prt^{gs} mutant oocytes and in wild types (Fig. 4C,D). However, we found a decreased OSK protein level when we performed anti-OSK antibody staining on developing oocytes and on whole-mount embryos originated from homozygous prt^{gs} females (Table 2 and Fig. 4E,F,J,K). Furthermore, confocal analysis of anti-OSK stained mutant ovaries revealed delocalised OSK protein in 15% of stage 10 oocytes (Fig. 4G-I). While OSK protein become concentrated at the posterior pole, the PRT-GFP aggregates concentrated at the subcortical region at stage 10 oocytes and showed colocalization with OSK protein at the posterior pole in wild type (Fig. 4L-N).

By western analysis, we also detected reduced OSK protein level in ovaries dissected from prt^{gs} homozygous females (Fig. 5). However, the decrease in the OSK protein level was exclusively due to reduction of the short OSK isoform, while the 71 kDa OSK isoform was virtually unaffected. In addition, we detected an alteration in the post-translational modification of the short OSK isoform (Fig. 5). The 55 kDa unphosphorylated short OSK isoform had almost disappeared and reduced amount of 57 kDa phosphorylated short OSK

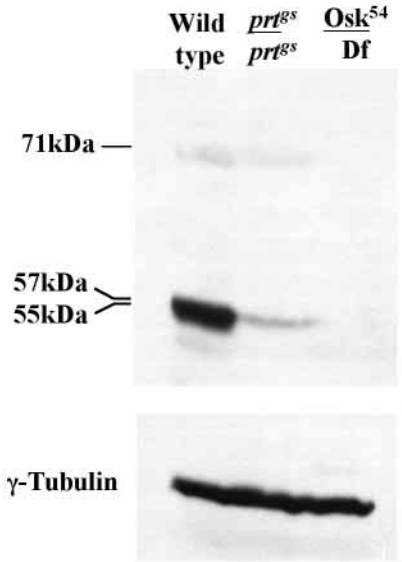

Fig. 5. Western blot analysis of prt^{gs} mutant ovaries. Western blot of ovary extracts probed with the anti-OSK antibody. Wild type, prt^{gs} and Osk^{54}/Df stands for an OSK protein null combination ($osk^{54}/Df(2)RPXT103$). The bottom panel shows the same Western blot probed with anti γ-Tubulin antibody as a loading control. The molecular weight of the three OSK-specific bands long OSK (71 kDa), phosphorylated short OSK (57 kDa) and unphosphorylated short OSK (55 kDa) are indicated.

isoform could be detected. These results strongly suggest that the *prt* gene acts at the short OSK protein level in the posterior gene hierarchy.

Prt and *Btk29A* interact genetically

The biochemical function of Sab, the human homologue of the *prt* gene has been revealed by in vitro and in vivo assays. The Sab protein preferentially binds to the Bruton's tyrosine kinase protein and negatively regulates its function (Matsushita et al., 1998; Yamadori et al., 1999). Because, theoretically, the absence of a negative regulator can be suppressed by decreasing the level of the regulated component, we tested whether hypomorphic *Btk* alleles can suppress prt^{gs} mutation. Recombinant chromosomes were generated from hypomorphic *Btk29A* mutations (*k00206, k05610* and *ficPL*) (Roulier et al., 1998; Baba et al., 1999), and null *pr t* mutation bearing chromosomes and double mutant females were tested for the grandchildless phenotype. We observed that the original 70% penetrant prt^{gs} homozygous phenotype was completely suppressed in $Btk29A^{ficPL}$ prt^{gs}/$Btk29A^{ficPL}$ prt^{gs}double mutant females, while in$Btk29A^{k05610}$ prt^{gs}/$Btk29A^{ficPL}prt^{gs}$and $Btk29A^{k00206}$ prt^{gs}/*Btk29A* prt^{gs} mutant females some residual gs phenotype, 4.4% and 4.0%, respectively, were measured. Thus, we concluded that *Prt* negatively regulates *Drosophila Btk*, because the *prt* null mutant phenotype is manifested only if *Btk* activity is present. To exclude the possibility that *Drosophila Btk29A* has, itself, a loss-of-function grandchildless phenotype, we repeated the $Btk29A^{k00206}$ and $Btk29A^{k05610}$ germline mosaic analyses published by Roulier (Roulier, 1998). Both $Btk29A^{k00206}$ and $Btk29A^{k05610}$ homozygous germline clones resulted in the earlier published loss-of-function, dumpless and maternal effect head defect phenotypes. We also found some normal looking eggs that were fertilised and developed to adulthood. Twenty such adult individuals were dissected in both experiments but no grandchildless gonad was found, indicating that *Btk29A* activity is not required for germline formation.

DISCUSSION

In this paper, we have identified the *prt* gene, which has an important role in the proper formation of embryonic germ cells in *Drosophila*. Null mutant of *prt* produces embryos that display a significant reduction in the number of germ cells, show a reduction of short OSK protein levels and abnormal OSK distribution. prt^{gs} and the BTK29A mutations were found to interact genetically. The PRT protein is found in large protein aggregates that are localised subcortically in the oocytes.

Posteriorly anchored OSK protein is a key component of the germ plasm and subsequent embryonic germ cell formation. Although, the anchoring process is an important aspect of *osk* regulation very little is known about its mechanism. Genetic analysis of the anchoring mechanism is especially difficult, as OSK anchoring is interdependent on the presence of both the mRNA and the protein at the posterior region (Glotzer et al., 1997; Markussen et al., 1995; Rongo et al., 1995). Therefore, mutations of regulatory genes that interfere with OSK protein localisation often also result in mRNA delocalisation, making it impossible to separate these two processes. An example of the above is provided by the *TmII* mutation, which abolishes the localisation of both *osk* mRNA and protein (Erdelyi et al., 1995; Tetzlaff et al., 1996). Therefore, the actin-binding TmII protein and the actin cytoskeleton may be directly connected, not only to the mRNA but also the OSK protein, at the posterior pole. Interestingly, in prt^{gs} mutants, the OSK protein delocalisation does not seem to be coupled with *osk* mRNA localisation. While *osk* mRNA was localised normally at the posterior pole in all stages of oogenesis, some OSK protein was detached from the subcortical region in prt^{gs}/prt^{gs} mutant ovaries. This delocalisation can reduce OSK concentration significantly at the posterior pole. The decreased OSK level leads to germ plasm reduction and the formation of fewer pole cells, which explain the *prt* mutant phenotype. As in early stages of oogenesis, OSK localisation seems completely normal and only becomes abnormal gradually during the subsequent stages, *prt* is very unlikely to interfere with OSK translation, rather it plays a role in OSK protein anchoring at the posterior pole or increases the stability of the anchored OSK protein.

In prt^{gs} mutants, only the short OSK isoform level was found to be reduced, while the long isoform remained at wild-type levels. This may explain the normal *osk* mRNA distribution, as the long OSK isoform can maintain its own mRNA at the posterior pole as described earlier (Markussen et al., 1995). However, the isoform specificity of prt^{gs} reveals that the two OSK isoforms may use independent posterior anchoring mechanisms or can be subjected to different post-translational regulation processes during their anchoring. However, genetic and molecular evidence suggests that some residual short OSK must still be present in prt^{gs} null mutants, because the complete loss of the short OSK isoform would not only result in grandchildless but rather a complete abdomen and germ cell-less phenotype (Markussen et al., 1995). This result also demonstrates that *prt* function in OSK anchoring must be redundant.

Subcellular localisation of PRT is reconcilable with *osk* regulatory function, because at the subcortical region their localisation overlaps. This colocalisation potentiates the functional interaction. Some *osk* translational regulatory proteins, which form a large ribonucleoprotein (RNP) complex, demonstrate a similar expression pattern during their transport to oocytes to that of PRT. Biochemical evidence exists that this RNP contains EXU and at least seven other proteins, in addition to *osk* and *bicoid* mRNAs (Wilsch-Brauninger et al., 1997; Wilhelm et al., 2000). We demonstrated that Exu, Orb and Me31 B, three elements of the above RNP complex, as well as CUP, an RNP independent protein with similar localisation pattern (Keyes and Spradling, 1997), are not colocalised with PRT in nurse cells. Consequently PRT aggregates, in spite of their similar subcellular localisation, have an independent transport system from either the EXU or the CUP complexes.

The genetic interaction found between *prt* and *Btk29A* indicates that the PRT regulatory function is evolutionary conserved. This is especially interesting, as the *Drosophila* BTK homologue is not required in germ cell formation. The Drosophila genome contains a single BTK homologue *Btk29A*, which encodes two protein species. *Btk29A* has several pleiotropic functions, such as male fertility and ring canal formation. It is expressed in the adult head, the larval immune

system, the male and female gonads, and several other tissues (Roulier et al., 1998; Baba et al., 1999; Vincent et al., 1989; Wadsworth et al., 1990). However, our germline clone analysis of the two hypomorhic alleles failed to reveal a role in germ cell formation. Based on the structural conservation of the Sab and PRT proteins, we anticipated that PRT might also exhibit a negative regulatory function similarly to Sab. According to this hypothesis, when PRT, the presumed negative regulator, is absent, an ectopic BTK activity would interfere with the normal function of the posterior gene hierarchy. Being normally suppressed, loss of function of such a negatively regulated gene would not be expected to cause any posterior phenotype. Indeed, the suppression of prt^{gs} phenotypes by hypomorphic *Btk29A* alleles indicates that in *Drosophila*, PRT also negatively regulates BTK29A.

Therefore, we propose that, in wild-type oocytes, PRT inactivates the BTK protein in the subcortical region. In prt^{gs} mutants, however, unregulated BTK interferes either with the localisation of subcortical cellular components in the oocyte, or it modifies the phosphorylation pattern of the short OSK protein itself. We find that the latter is a less feasible explanation, because in prt^{gs} mutants we do not find increased levels of phosphorylated short OSK that would be the result of extra kinase activity, instead the level of 57 kDa phosphorylated short OSK isoform is also significantly reduced. We suggest that uncontrolled BTK kinase activity modifies the anchoring capability of short OSK directly or indirectly to the subcortical region, resulting in delocalisation and degradation of both phosphorylated and unphosphorylated short OSK proteins. Because only the phosphorylated short OSK isoform was detected in prt^{gs} mutants, we suppose that either this protein is more stable or it is better anchored to the posterior pole, compared with the unphosphorylated one. The weakly anchored OSK protein is displaced by the cytoplasmic streaming and loses its pole plasm organising activity. Future research should be directed towards determining the precise biochemical function of PRT and elucidating the anchoring mechanism of OSK protein.

We thank Anne Ephrussi for providing *osk* cDNA, anti-OSK and anti-VAS and anti-STAU antibodies. We are grateful for Satoru Kobayashi for anti-Me31 B, Allan Spradling for anti-CUP, Christiane Nüsslein-Volhard for anti-Exu antisera. We thank Steven Beckendorf for FRT-*Btk*, Daisuke Yamamoto for fic^{P} mutant lines and Juergen Knoblich for β-globin-2xGFP vector. We are also grateful to Selen Muratoglu for molecular technical help, and to Barbara Botos, Mim Bower and the BRC Drosophila Community for critical reading of the manuscript. The work was supported by a grant (T22096) from the Hungarian National Science Foundation (OTKA). *prt* gene has been named after the famous detective Hercule Poirot.

REFERENCES

Adams, M. D., Celniker, S. E., Holt, R. A., Evans, C. A., Gocayne, J. D., Amanatides, P. G., Scherer, S. E., Li, P. W., Hoskins, R. A., Galle, R. F. et al. (2000). The genome sequence of Drosophila melanogaster. *Science* **287**, 2185-2195.

Baba, K., Takeshita, A., Majima, K., Ueda, R., Kondo, S., Juni, N. and Yamamoto, D. (1999). The Drosophila Bruton's tyrosine kinase (Btk) homolog is required for adult survival and male genital formation. *Mol. Cell Biol.* **19**, 4405-4413.

Bergsten, S. E. and Gavis, E. R. (1999). Role for mRNA localization in translational activation but not spatial restriction of nanos RNA. *Development* **126**, 659-669.

Breitwieser, W., Markussen, F. H., Horstmann, H. and Ephrussi, A. (1996). Oskar protein interaction with Vasa represents an essential step in polar granule assembly. *Genes Dev.* **10**, 2179-2188.

Calvi, B. R., Hong, T. J., Findley, S. D. and Gelbart, W. M. (1991). Evidence for a common evolutionary origin of inverted repeat transposons in Drosophila and plants: hobo, Activator, and Tam3. *Cell* **66**, 465-471.

Chang, J. S., Tan, L. and Schedl, P. (1999). The Drosophila CPEB homolog, orb, is required for oskar protein expression in oocytes. *Dev. Biol.* **215**, 91-106.

Cooperstock, R. L. and Lipshitz, H. D. (2001). RNA localization and translational regulation during axis specification in the Drosophila oocyte. *Int. Rev. Cytol.* **203**, 541-566.

Dahanukar, A., Walker, J. A. and Wharton, R. P. (1999). Smaug, a novel RNA-binding protein that operates a translational switch in Drosophila. *Mol. Cell* **4**, 209-218.

Dahanukar, A. and Wharton, R. P. (1996). The Nanos gradient in Drosophila embryos is generated by translational regulation. *Genes Dev.* **10**, 2610-2620.

Ephrussi, A., Dickinson, L. K. and Lehmann, R. (1991). Oskar organizes the germ plasm and directs localization of the posterior determinant nanos. *Cell* **66**, 37-50.

Ephrussi, A. and Lehmann, R. (1992). Induction of germ cell formation by oskar. *Nature* **358**, 387-392.

Erdélyi, M., Michon, A. M., Guichet, A., Glotzer, J. B. and Ephrussi, A. (1995). Requirement for Drosophila cytoplasmic tropomyosin in oskar mRNA localization. *Nature* **377**, 524-527.

Gavis, E. R. and Lehmann, R. (1994). Translational regulation of nanos by RNA localization. *Nature* **369**, 315-318.

Glotzer, J. B., Saffrich, R., Glotzer, M. and Ephrussi, A. (1997). Cytoplasmic flows localize injected oskar RNA in Drosophila oocytes. *Curr. Biol.* **7**, 326-337.

Gunkel, N., Yano, T., Markussen, F. H., Olsen, L. C. and Ephrussi, A. (1998). Localization-dependent translation requires a functional interaction between the 5′ and 3′ ends of oskar mRNA. *Genes Dev.* **12**, 1652-1664.

Hartl, D. L., Nurminsky, D. I., Jones, R. W. and Lozovskaya, E. R. (1994). Genome structure and evolution in Drosophila: applications of the framework P1 map. *Proc. Natl. Acad. Sci. USA* **91**, 6824-6829.

Jankovics, F., Sinka, R. and Erdelyi, M. (2001). An interaction type of genetic screen reveals a role of the Rab11 gene in oskar mRNA localization in the developing Drosophila oocyte. *Genetics* **158**, 1177-1188.

Keyes, L. N. and Spradling, A. C. (1997). The Drosophila gene fs(2)cup interacts with otu to define a cytoplasmic pathway required for the structure and function of germ-line chromosomes. *Development* **124**, 1419-1431.

Kim-Ha, J., Smith, J. L. and Macdonald, P. M. (1991). oskar mRNA is localized to the posterior pole of the Drosophila oocyte. *Cell* **66**, 23-35.

Kim-Ha, J., Kerr, K. and Macdonald, P. M. (1995). Translational regulation of oskar mRNA by bruno, an ovarian RNA-binding protein, is essential. *Cell* **81**, 403-412.

Kimmerly, W., Stultz, K., Lewis, S., Lewis, K., Lustre, V., Romero, R., Benke, J., Sun, D., Shirley, G., Martin, C. and Palazzolo, M. (1996). A P1-based physical map of the Drosophila euchromatic genome. *Genome Res.* **6**, 414-430.

Lie, Y. S. and Macdonald, P. M. (1999). Apontic binds the translational repressor Bruno and is implicated in regulation of oskar mRNA translation. *Development* **126**, 1129-1138.

Lindsley, D. L. and Zimm, G. G. (1992). *The Genome of* Drosophila melanogaster. Sane Diego: Academic Press

Mansfield, J. H., Wilhelm, J. E. and Hazelrigg, T. (2002). Ypsilon Schachtel, a Drosophila Y-box protein, acts antagonistically to Orb in the oskar mRNA localization and translation pathway. *Development* **129**, 197-209.

Markussen, F. H., Michon, A. M., Breitwieser, W. and Ephrussi, A. (1995). Translational control of oskar generates short OSK, the isoform that induces pole plasma assembly. *Development* **121**, 3723-3732.

Matsushita, M., Yamadori, T., Kato, S., Takemoto, Y., Inazawa, J., Baba, Y., Hashimoto, S., Sekine, S., Arai, S. and Kunikata, T. (1998). Identification and characterization of a novel SH3-domain binding protein, Sab, which preferentially associates with Bruton's tyrosine kinase (BtK). *Biochem. Biophys. Res. Commun.* **245**, 337-343.

Micklem, D. R., Adams, J., Grunert, S. and St Johnston, D. (2000). Distinct roles of two conserved Staufen domains in oskar mRNA localization and translation. *EMBO J.* **19**, 1366-1377.

Nakamura, A., Amikura, R., Hanyu, K. and Kobayashi, S. (2001). Me31B

silences translation of oocyte-localizing RNAs through the formation of cytoplasmic RNP complex during Drosophila oogenesis. *Development* **128**, 3233-3242.

Rongo, C., Gavis, E. R. and Lehmann, R. (1995). Localization of oskar RNA regulates oskar translation and requires Oskar protein. *Development* **121**, 2737-2746.

Rorth, P. (1998). Gal4 in the Drosophila female germline. *Mech. Dev.* **78**, 113-118.

Roulier, E. M., Panzer, S. and Beckendorf, S. K. (1998). The Tec29 tyrosine kinase is required during Drosophila embryogenesis and interacts with Src64 in ring canal development. *Mol. Cell* **1**, 819-829.

Rubin, G. M. and Spradling, A. C. (1982). Genetic transformation of Drosophila with transposable element vectors. *Science* **218**, 348-353.

Rubin, G. M., Hong, L., Brokstein, P., Evans-Holm, M., Frise, E., Stapleton, M. and Harvey, D. A. (2000). A Drosophila complementary DNA resource. *Science* **287**, 2222-2224.

Saffman, E. E., Styhler, S., Rother, K., Li, W., Richard, S. and Lasko, P. (1998). Premature translation of oskar in oocytes lacking the RNA-binding protein bicaudal-C. *Mol. Cell Biol.* **18**, 4855-4862.

Salles, F. J., Lieberfarb, M. E., Wreden, C., Gergen, J. P. and Strickland, S. (1994). Coordinate initiation of Drosophila development by regulated polyadenylation of maternal messenger RNAs. *Science* **266**, 1996-1999.

Smibert, C. A., Wilson, J. E., Kerr, K. and Macdonald, P. M. (1996). smaug protein represses translation of unlocalized nanos mRNA in the Drosophila embryo *Genes Dev*. **10**, 2600-2609.

Smith, D., Wohlgemuth, J., Calvi, B. R., Franklin, I. and Gelbart, W. M. (1993). hobo enhancer trapping mutagenesis in Drosophila reveals an insertion specificity different from P elements. *Genetics* **135**, 1063-1076.

Smith, J. L., Wilson, J. E. and Macdonald, P. M. (1992). Overexpression of oskar directs ectopic activation of nanos and presumptive pole cell formation in Drosophila embryos. *Cell* **70**, 849-859.

St Johnston, D., Beuchle, D. and Nüsslein-Volhard, C. (1991). Staufen, a gene required to localize maternal RNAs in the Drosophila egg. *Cell* **66**, 51-63.

Tetzlaff, M. T., Jackle, H. and Pankratz, M. J. (1996). Lack of Drosophila cytoskeletal tropomyosin affects head morphogenesis and the accumulation of oskar mRNA required for germ cell formation. *EMBO J.* **15**, 1247-1254.

Underwood, E. M., Briot, A. S., Doll, K. Z., Ludwiczak, R. L., Otteson, D. C., Tower, J., Vessey, K. B. and Yu, K. (1990). Genetics of 51D-52A, a region containing several maternal-effect genes and two maternal-specific transcripts in Drosophila. *Genetics* **126**, 639-650.

Van Doren, M., Williamson, A. L. and Lehmann, R. (1998). Regulation of zygotic gene expression in Drosophila primordial germ cells. *Curr. Biol.* **8**, 243-246.

Vincent, W. S., III, Gregory, R. J. and Wadsworth, S. C. (1989). Embryonic expression of a Drosophila src gene: alternate forms of the protein are expressed in segmental stripes and in the nervous system. *Genes Dev.* **3**, 334-347.

Wadsworth, S. C., Muckenthaler, F. A. and Vincent, W. S., III (1990). Differential expression of alternate forms of a Drosophila src protein during embryonic and larval tissue differentiation. *Dev. Biol.* **138**, 296-312.

Webster, P. J., Liang, L., Berg, C. A., Lasko, P. and Macdonald, P. M. (1997). Translational repressor bruno plays multiple roles in development and is widely conserved. *Genes Dev.* **11**, 2510-2521.

Wieshaus, E. and Nüsslein-Volhard, C. (1986). Looking at embryos. In Drosophil*a: A Practical Approach*, pp. 199-227. Oxford: IRL Press.

Wilhelm, J. E., Mansfield, J., Hom-Booher, N., Wang, S., Turck, C. W., Hazelrigg, T. and Vale, R. D. (2000). Isolation of a ribonucleoprotein complex involved in mRNA localization in Drosophila oocytes. *J. Cell Biol.* **148**, 427-440.

Wilsch-Brauninger, M., Schwarz, H. and Nüsslein-Volhard, C. (1997). A sponge-like structure involved in the association and transport of maternal products during Drosophila oogenesis. *J. Cell Biol.* **139**, 817-829.

Wilson, J. E., Connell, J. E. and Macdonald, P. M. (1996). aubergine enhances oskar translation in the Drosophila ovary. *Development* **122**, 1631-1639.

Yamadori, T., Baba, Y., Matsushita, M., Hashimoto, S., Kurosaki, M., Kurosaki, T., Kishimoto, T. and Tsukada, S. (1999). Bruton's tyrosine kinase activity is negatively regulated by Sab, the Btk-SH3 domain-binding protein. *Proc. Natl. Acad. Sci. USA* **96**, 6341-6346.